

1. INTRODUCTION AND EXPLANATORY NOTES¹

Shipboard Scientific Party²

BACKGROUND AND OBJECTIVES

Deep Sea Drilling Project (DSDP) Legs 64 and 65 were planned as a coordinated drilling investigation of the Gulf of California. The primary goals of Leg 64 were to investigate the early evolution of a passive continental margin and to study hydrothermal systems in the Guaymas Basin. Leg 65 was designed to study the processes of crustal accretion along the relatively fast-spreading East Pacific Rise for comparison with the slow-spreading Mid-Atlantic Ridge.

The Gulf of California is one of the few modern examples of a young rifted ocean basin and has several unique features which make it an ideal environment for deep basement drilling. It is believed to have formed during the past 3 to 4 m.y. by the splitting of Baja California away from the Mexican mainland. During early Tertiary time, prior to approximately 25 m.y. ago, the entire western margin of North America was marked by a subduction zone along which oceanic lithosphere was underthrust beneath the continent (Atwater, 1970). Subduction of the Farallon Plate continued until the North American and Pacific Plates collided in the present-day vicinity of San Francisco. The San Andreas transform fault then developed as the triple junction migrated southward from the initial point of plate collision. Approximately 4 to 4.5 m.y. ago the spreading center jumped inland, causing Baja California to begin rifting away from mainland Mexico.

The present structure and bathymetry of the Gulf of California express this evolving tectonic pattern. The crest of the East Pacific Rise extends northward more or

less continuously to the Tamayo Fracture Zone at the mouth of the Gulf. North of the Tamayo Fracture Zone, the rise is broken into a series of small spreading centers offset by increasingly frequent transform faults oriented obliquely to the axis of the Gulf (Fig. 1). The spreading centers are expressed bathymetrically as deep basins which are partially filled with variable thicknesses of sediment derived from the adjacent land masses. New ocean crust is currently being formed along the crest of the East Pacific Rise and along the short spreading segments within the Gulf itself. Thus, the Gulf of California represents a transition zone between a predominantly spreading environment on the south to a predominantly transform environment on the north. Axial spreading in the Gulf occurs at a rate of about 6 cm per year.

Ambient sedimentation rates are extremely high at the northern end of the Gulf where the Colorado River delta is presently being formed. The rates generally decrease to the south, but even at the mouth of the Gulf they are much higher than in older ocean basins. As a result the newly formed oceanic basement in the Gulf was thought to have formed largely by intrusion into a

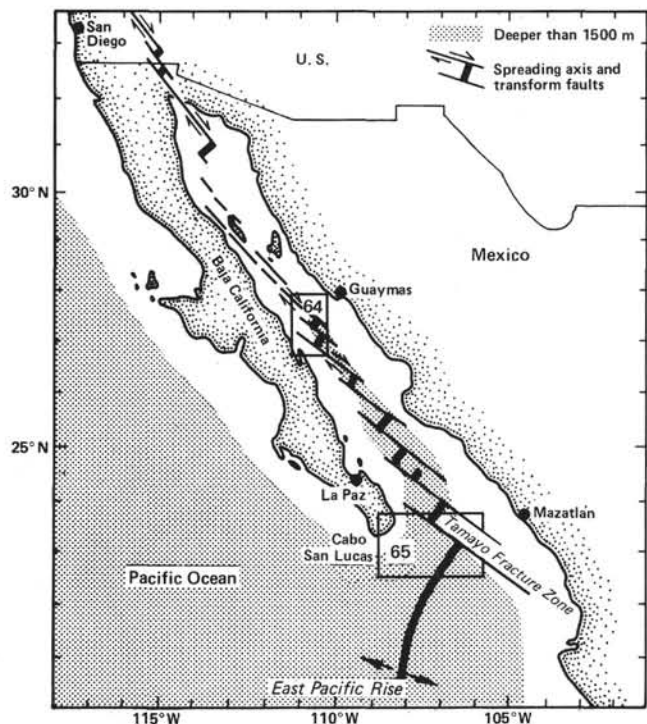


Figure 1. Tectonic setting of areas drilled on Legs 64 and 65 in the Gulf of California.

¹ Lewis, B. T. R., Robinson, P., et al., *Init. Repts. DSDP, 65*; Washington (U.S. Govt. Printing Office).

² Brian T. R. Lewis (Co-Chief Scientist), Department of Oceanography, University of Washington, Seattle, Washington; Paul T. Robinson (Co-Chief Scientist), Department of Earth Sciences, University of California, Riverside, California (present address: Department of Geology, Dalhousie University, Halifax, Nova Scotia, Canada); Richard N. Benson, Delaware Geological Survey, University of Delaware, Newark, Delaware; Grant Blackinton, Hawaii Institute of Geophysics, University of Hawaii at Manoa, Honolulu, Hawaii; Ron Day, Department of Geological Sciences, University of California, Santa Barbara, California (present address: Arco Oil and Gas Company, Dallas, Texas); Frederick K. Duenneber, Hawaii Institute of Geophysics, University of Hawaii at Manoa, Honolulu, Hawaii; Martin Flower, Department of Mineral Sciences, Museum of Natural History, Smithsonian Institution, Washington, D.C. (present address: Department of Geological Sciences, University of Illinois at Chicago Circle, Chicago, Illinois); Mario Gutiérrez-Estrada, Instituto de Ciencias del Mar y Limnología, Universidad Nacional Autónoma de México, Mexico City, Mexico (present address: Estación de Investigaciones Mazatlán, Universidad Nacional Autónoma de México, Mazatlán, Sinaloa, Mexico); John Hattner, Department of Geology, Florida State University, Tallahassee, Florida (present address: Chevron Oil Company, Lafayette, Louisiana); Albert M. Kudo, Department of Geology, University of New Mexico, Albuquerque, New Mexico; M. Ann Morrison, Department of Geology, Imperial College, London, England (present address: Department of Geological Sciences, University of Birmingham, Birmingham, England); Claude Rangin, Laboratoire Tectonique, Université Pierre et Marie Curie, Paris, France; Matthew H. Salisbury, Deep Sea Drilling Project, Scripps Institution of Oceanography, La Jolla, California; Hans-Ulrich Schmincke, Institut für Mineralogie, Ruhr-Universität, Bochum, Federal Republic of Germany; Ralph Stephen, Department of Geology and Geophysics, Woods Hole Oceanographic Institution, Woods Hole, Massachusetts; Boris P. Zolotarev, Geological Institute, U.S.S.R. Academy of Sciences, Moscow, U.S.S.R.

thick sedimentary pile rather than by extrusion onto the seafloor. Since the high sedimentation rates result from the proximity of continental land masses, this type of ocean crust is probably common in young ocean basins formed by rifting of continental crust, and may be characteristic of many passive margins.

On Leg 65 it was planned to drill a transect across the East Pacific Rise just south of the Tamayo Fracture Zone and to penetrate deep into the crust at one site near the ridge crest. The purpose was to sample crustal sections formed at a relatively fast spreading ridge in order to investigate the processes of crustal accretion in this environment. On earlier Legs (37, 45, 46, 49), it was found that crustal sections formed at the slow-spreading Mid-Atlantic Ridge are characterized by significant structural and lithologic heterogeneity. Crustal construction processes are highly episodic, and there is evidence of extensive crystal fractionation in closed magma systems. Fast-spreading ridges, on the other hand, are commonly thought to produce simpler crustal sections formed by more continuous rifting and eruption. Many models suggest the presence of large, open, continuously evolving magma chambers beneath fast-spreading ridges in which extensive magma mixing takes place. However, such models had not been tested by actual sampling of accreted sections. Attempts to drill young crust in the eastern Pacific on Legs 34 and 54 failed to penetrate significant sections of igneous basement because of the highly fractured nature of the rocks. The deep drilling target at the mouth of the Gulf was selected because the basement seismic velocities there are relatively high (about 5 km/s), i.e., comparable to those of the old, cemented, and sealed North Atlantic basement drilled successfully at Sites 417 and 418 (Donnelly et al., 1980). The high velocities suggested either that the crust at the mouth of the Gulf is relatively unfractured or that the fractures have been sealed by secondary minerals. In addition, the high sedimentation rates along this part of the East Pacific Rise make it possible to spud into nearly "zero age" basement. Zero-age drilling is necessary in order to examine some of the more ephemeral properties of near-axis oceanic crust, such as heat flow, hydrothermal flux, and seismicity.

Detailed surveying across the northern end of the East Pacific Rise during the IPOD site surveys revealed a pattern of alternating ridges and flat-floored valleys, symmetrically disposed on opposite sides of the rise crest (Fig. 2) (Lewis et al., this volume). The ridges are discontinuous linear features extending parallel to the rise crest for distances of 5 to 30 km. Dredging of these features has indicated that they are composed largely of pillow lavas. The intervening valleys are underlain by variable thicknesses of sediments which seismic reflection profiles show to be tectonically undisturbed. The basement/sediment interface is smooth, tilts slightly away from the Rise axis, and shows no evidence of faulting. Because of the need to spud in sediments, all of the sites planned for Leg 65 were located within these valleys.

Two holes in the transect had already been drilled on Legs 63 (Site 473) and 64 (Site 474). Forty meters of basement were penetrated at Site 473 and a 105-meter-

thick basement section was sampled at Site 474. Drilling at this site revealed an upper sequence composed of interlayered massive basalts and sediments, below which was found a section of interlayered pillowed and massive basalts. The uppermost massive units are compositionally distinct from the lower basement section and were thought to represent late stage sills emplaced during a period of off-axis volcanic activity.

The final sites selected for Leg 65 were designed not only to test models for crustal accretion at the rift axis but to make possible several downhole experiments. It was planned, for example, to emplace a downhole seismometer developed by the Hawaii Institute of Geophysics in a hole near the ridge crest in order to monitor natural seismicity along the spreading axis. An oblique seismic experiment was also planned at one site as a means of determining the structure of the upper basement layers.

ORGANIZATION

The results of Leg 65 are presented in two sections. The first describes the geophysical surveys conducted in the area of the drill sites, the detailed results of drilling at each site, and the results of special geophysical studies (downhole logging and seismic experiments) carried out in conjunction with the drilling program. The second section contains chapters that discuss extensively the results of shorebased investigations and synthesis chapters for the entire leg. A foldout at the back of the volume ("Bathymetric Map of the Tamayo Transform Fault") shows the results of a Seabeam survey conducted in the area after the drilling had been completed.

AUTHORSHIP

In general, the material presented in the site summaries was prepared by the Shipboard Scientific Party. Although most of the data were obtained on shipboard, the geochemical analyses were supplemented by shore-based personnel, Na₂O analyses were obtained by P. Cambon, and the paleomagnetic data for Holes 483B and C and Site 485 were measured on shore with the assistance of M. Osterhoudt and U. Bleil.

SURVEY AND DRILLING DATA

Survey data crucial to site selection and hole positioning are presented in the various site reports. While steaming between sites, continuous profiles of depth, total magnetic field, and sub-bottom seismic reflections were taken. Before dropping the beacon at each site, we made short surveys using a precision echo sounder, a seismic profiler, and a proton precision magnetometer.

Underway depths were recorded continuously on an EDO-Western precision graphic recorder. The depths were read in meters, assuming a sound velocity in water of 1500 m/s. The seafloor depth at each site was corrected both for variations in sound velocity using the tables presented by Matthews (1939) and for the depth of the echo-sounder transducer (6 m). In addition, all depths given with respect to the drilling platform were calculated assuming a distance of 10 meters between the floor of the drilling platform and the water line.

NW

SE

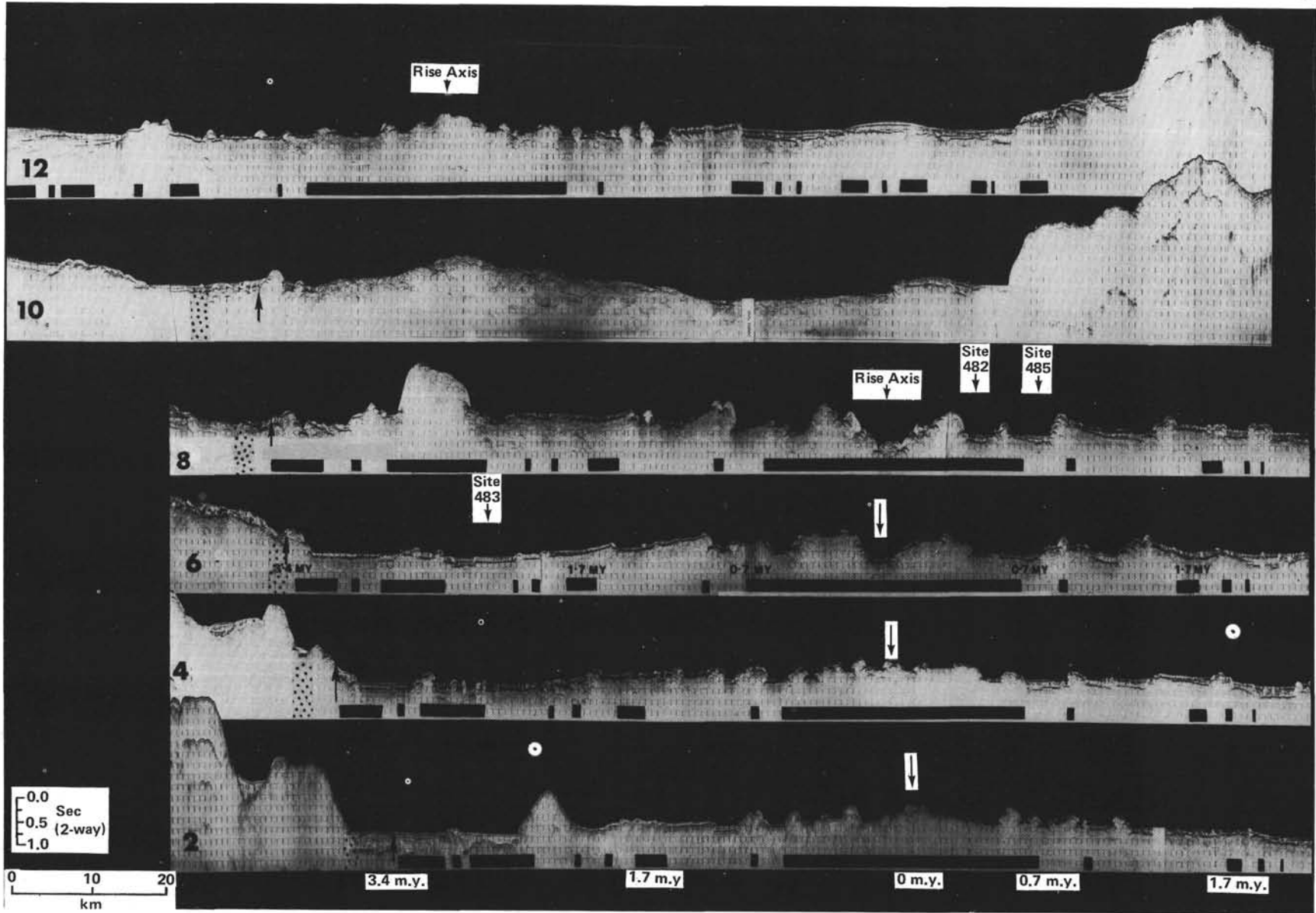


Figure 2. Seismic reflection profiles across the mouth of the Gulf of California. Profiles are arranged sequentially from north (12) to south (2) (after Lewis et al., this volume).

The seismic reflection profiling system used consisted of two Bolt air guns, a Scripps-designed hydrophone array, Bolt amplifiers, two band-pass filters, and two EDO dry-paper recorders; the two recording systems normally operated at different scales and filter settings. Copies of the underway data may be obtained from the manager of the data library, at the Deep Sea Drilling Project, Scripps Institution of Oceanography, La Jolla, California.

SHIPBOARD PROCEDURES

Numbering Conventions and Core-Handling Procedures

The drill sites have been numbered consecutively from the first site drilled by the *Glomar Challenger* in 1968. The first (or only) hole drilled at a given site is assigned the site number; if more holes are drilled at the same site, the second is identified by the site number and the suffix A, the third by the site number and the suffix B, and so on.

The cores from each hole are numbered sequentially from the top down. In the ideal case (Fig. 3), each core consists of 9.5 meters of sediment or rock in a plastic liner 6.6 cm in diameter. In addition, a 20-cm long sample may be obtained from the core catcher (a multi-fingered device at the bottom of the core barrel that prevents cored material from sliding out of the core barrel while it is being brought to the surface) or, more rarely, from the bit itself. These samples represent the lowest material recovered in each core. The cored interval for each core is the interval in meters below the seafloor measured from the point at which the coring was started to the point at which it was terminated. The interval is generally about 9.5 meters long (the nominal length of a core barrel), but may be shorter or longer depending upon the circumstances of drilling.

When a core and its enclosing liner are brought aboard the *Glomar Challenger*, they are cut into 1.5-meter-long sections, sealed, labeled, and moved into the core laboratory for processing. A full 9.5-meter-long core (including core catcher) consists of seven sections, numbered 1 through 7 from the top down. If less than 9.5 meters is recovered, the sections are still numbered starting with 1 at the top, but the number of sections is the number of 1.5-meter-long intervals needed to accommodate the length of core recovered. In such cases, the core recovery is measured from the top of the recovered material, with the top of Section 1 set equal to the top of the cored interval. Figure 3 illustrates the possible core configurations and the section-labeling procedure.

After an initial assessment of the age of the sediments in the core catcher and the wet-bulk density and porosity of the core have been determined by GRAPE (gamma-ray attenuation) analysis, each 1.5-meter section is split longitudinally into an "archive" half and a "working" half. The former is photographed and described in terms of composition, color, texture, and structure as will be discussed. The working half, after sampling for

shipboard determination of grain size, carbon-carbonate, and water content, as well as for paleontological and physical property studies, is further sampled for subsequent shore-based analysis. Each sample taken from the core is designated by the interval, in centimeters, from the top of the section from which the sample was extracted; the sample volume, in cm^3 , is also noted. Thus, a full sample designation consists of the following information:

Leg (optional)

Site

Hole

Core

Section

Interval in centimeters from the top of the section

Sample size in cm^3

Thus, Sample 65-483B-9-3, 12-14 cm (10 cm^3) designates a 10-cm^3 sample taken from Section 3 of Core 9 from the third hole (Hole B) drilled at Site 483. The depth below the seafloor for this sample would be the depth to the top of the core plus 3 meters for Sections 1 and 2, plus 12 cm (depth below the top of Section 3), or 3.12 meters.

After the sediment cores are described and sampled, they are maintained in cold storage on the ship until they are transferred to one of the Deep Sea Drilling Project (DSDP) repositories (in this case, the West Coast Repository at the Scripps Institution of Oceanography, La Jolla, California).

The handling of hard-rock material (e.g., basaltic rock) differs slightly from that of sediment cores. After the core has been cut into 1.5-meter long sections and split with a rock saw into working and archive halves, the rocks are examined and thin Styrofoam spacers are placed between those that cannot be fitted back together. The rocks are subdivided by this means into pieces which are numbered sequentially from the top of each section. If a piece consists of several fragments that fit together, these may be further identified by letter suffixes starting from the top of the piece (e.g., 8a, 8b, etc.). In practice, the spacers are used most often in basalt sequences to delineate intervals of no recovery or to indicate voids between pillows and in breccias. Since the thickness of the spacers is finite and arbitrary (about 0.5 cm), their insertion increases the apparent recovery. If, for any reason, it is necessary to determine the position of a sample in a core prior to the insertion of the spacers, the cumulative thickness of the spacers overlying the sample must be subtracted from its apparent depth.

After the identification of each piece with a label indicating the hole, core, section, interval, piece, and orientation (if unambiguous), the archive half is described, photographed, and placed in shrink tubing. The working half is then sampled for shipboard geochemical, magnetic, physical property, and thin-section studies, and for subsequent shore-based analysis. After the cores have been described and sampled, they are maintained in cold storage on board until transfer to the repository.

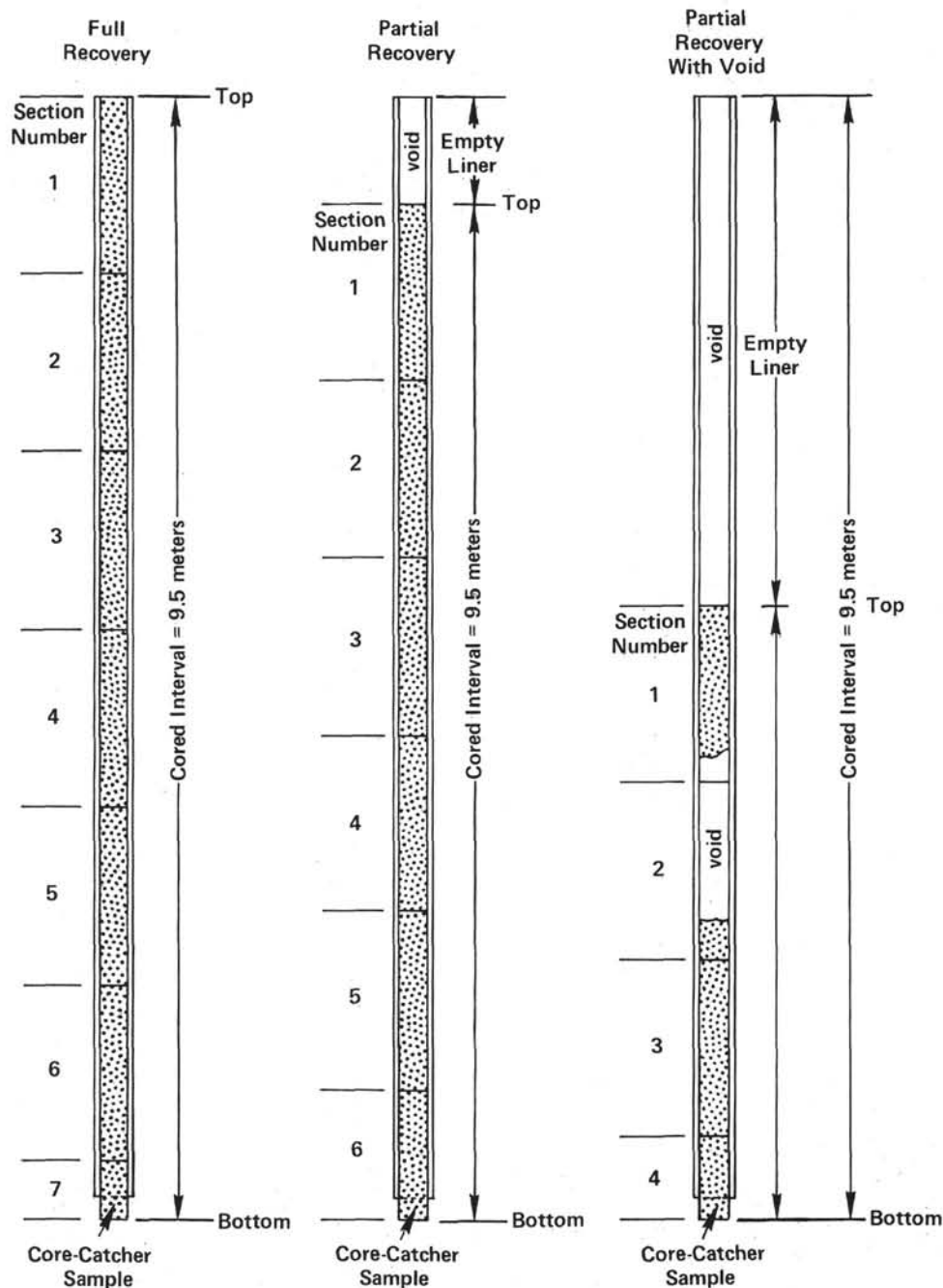


Figure 3. Labeling of sections for various recovery configurations.

SHIPBOARD MEASUREMENT PROCEDURES

Physical Properties

A thorough discussion of the procedures used on shipboard to measure physical properties is given by Boyce (1973); we will offer only a brief review here.

1) The density and porosity of the samples recovered on Leg 65 were measured by both gravimetric and gamma-ray attenuation (GRAPE) techniques. The gravimetric measurements were made on coherent samples using the immersion method and a simple beam balance; after the wet-bulk density of each sample had been determined from its mass and volume, each sample was

dried and reweighed in order to determine its porosity and grain density. Since the balance could be read to ± 0.01 g and the samples typically weighed about 30 g, the wet-bulk density measurements are considered accurate to better than 1%. The porosity measurements are considered less accurate, as a result of incomplete desiccation.

The GRAPE measurements were made on selected coherent samples using the 2-minute counting technique and on full sections of core using both the 2-minute and the continuous counting procedure (see Boyce, 1973). The method makes use of Compton scattering of gamma rays by electrons in the sample to measure the elec-

iron density of the sample, from which may be inferred the bulk density of the sample. The gamma-ray source used aboard the *Glomar Challenger* is ^{133}Ba , which emits gamma rays with energies of 0.300 and 0.359 MeV. The gamma rays are scattered such that the beam intensity is given by the relation:

$$I = I_0 e^{-\mu \rho_b d}$$

where I is the measured beam intensity through the sample, I_0 is the initial intensity (no sample), μ is the Compton mass attenuation coefficient (0.1024 cm^2/g for quartz), and ρ_b is the apparent bulk density of the sample. Thus one can obtain an approximate value for the bulk density of the sample from the relation,

$$\rho_b = \frac{\ln(I_0/I)}{\mu d}$$

where d is the sample thickness. No corrections have been made for variations in composition. The porosity, ϕ , of each sample was determined from the relation,

$$\phi = \frac{\rho_g - \rho_b}{\rho_g - \rho_f}$$

where ρ_g is the estimated average grain density of the sample and ρ_f is the density of the interstitial fluid (assumed to be 1.025 g/cm^3 , the density of seawater).

2) The compressional-wave velocity of the samples was determined at atmospheric pressure using a Hamilton Frame velocimeter. The velocity is obtained by measuring the time of flight of a 400-kHz sonic pulse through a sample set between two transducers and measuring the thickness of the sample with a dial gauge.

3) The shear strength of the sediments recovered on Leg 65 was measured at room temperature and pressure using a Soiltest Torvane shear-strength meter with its axis of rotation aligned parallel to bedding. Since many of the samples measured had been disturbed during drilling, the values obtained can only be considered qualitatively correct.

4) The thermal conductivity of the sediments was measured to $\pm 4\%$ using the needle-probe technique described by Von Herzen and Maxwell (1959). From three to five measurements were typically made 20 to 30 cm apart in each section examined. All measurements were made after the core had been allowed to equilibrate to room temperature.

Geochemical Measurements

The pH, alkalinity, chlorinity, salinity, and Ca^{2+} and Mg^{2+} contents of the recovered sediments were measured routinely on the ship.

1) The pH was determined by a flow-through electrode method in which a small portion of unfiltered water is passed through a glass capillary electrode.

2) The alkalinity was measured by colorimetric titration of a 1-ml aliquot of interstitial water with 0.1N HCl, using methyl red/blue indicator, and the relation

$$\text{Alkalinity (meq/kg)} = (\text{ml HCl titrated}) \cdot (97.752)$$

3) Salinity was calculated from the fluid refractive index as measured by a Goldberg optical refractometer, using the ratio,

$$\text{Salinity (\%)} = (0.55) \Delta N,$$

where ΔN = refractive index difference $\times 10^4$. Local surface seawater was regularly examined by each of the above methods to provide a reference for comparison.

Sediment Analyses

1. Shipboard carbonate analyses were done by the "Karbonate Bombe" technique of Müller and Gastner (1971). In this procedure, a powdered sample is treated with HCl in a closed cylinder. The resulting CO_2 pressure is proportional to the amount of CaCO_3 in the sample. The technique is considered accurate to ± 2 to $\pm 5\%$.

2. Measurements of the organic carbon content of selected samples were made on board ship using a Hewlett-Packard CHN analyzer.

3. The carbon-carbonate data were determined at the DSDP sediment laboratory in La Jolla using a LECO induction furnace combined with a LECO acid-base semi-automatic carbon determinator. Step-by-step procedures are presented in Volume 4 of the *Initial Reports of the Deep Sea Drilling Project*, and the methods, calibration, accuracy, and precision of the technique are discussed in Volume 9.

4. The grain-size distribution of the sediments was determined at the DSDP sediment laboratory by standard sieve and pipette analysis using the procedures outlined in Volume 5 of the *Initial Reports*. In general, the sand-, silt-, and clay-size fractions are reproducible to within $\pm 2.5\%$ (absolute). There is a discussion of this precision in Volume 9 in the *Initial Reports*.

Paleomagnetic Measurements

The magnetic properties of the samples recovered on Leg 65 were measured on shipboard using a Digico balanced fluxgate magnetometer and a Schönstedt alternating-field (AF) specimen demagnetizer. The properties determined include the NRM intensity and inclination, the stable inclination, and the median demagnetizing field of the basalts. In addition, the initial susceptibility field of a number of samples was studied using a Bison 3101 magnetic susceptibility meter.

The specimens examined were cut in the form of 1-inch cylindrical mini-cores aligned perpendicular to the drill string with an orientation arrow drawn on one face to indicate the vertical direction. This arrow is equivalent to the fiducial line used to orient the sample in the spinner and points in the direction of the positive x-component of magnetization. The positive y-component is perpendicular to x in the plane of the flat face and is directed to the right, while the positive z-component is directed away from the flat face along the axis of the minicore. To restore the measured magnetic vector to its

original vertical orientation (the azimuthal orientation remains unknown) a bedding correction in the Digico program is used to carry out a 90° rotation.

The magnetometer was calibrated for intensity and direction using a shipboard Digico standard and three standards brought aboard for the leg. These standards, in turn, were calibrated against measurements made on two magnetometers at the University of California at Santa Barbara. The calibration was checked frequently during the measurements (at least once per hour) because the measured intensity was found to drift (apparently at random) at a rate of about 0.2% per hour. The direction of magnetization could be reproduced to within 0.5° but care was needed when positioning the sample in the magnetometer. The noise intensity level was always less than 10^{-6} emu/cm³ and was usually less than 10^{-7} emu/cm³.

The Schönstedt alternating-field demagnetizer was used to demagnetize the samples in order to determine the median demagnetizing field and stable inclination of the basalts. The ambient direct field inside the demagnetizer coil (measured using a portable fluxgate magnetometer) was 150γ at an alternating field intensity of 0.0 Oe and rose to 300γ at the maximum intensity of 1000 Oe. The calibration of the demagnetizer was found to be high by about 2%.

The magnetic susceptibility meter was used to measure the weak field susceptibility of the samples. The minicores used on board were shorter than those required for the correct calibration of the susceptibility meter. The correction factor given in the Bison instrument manual is:

$$\frac{\text{Sample holder length}}{\text{Sample length}} = \frac{5.0}{\text{Sample length}}$$

However, a calibration check on Leg 65 showed that:

$$\frac{4.4}{\text{Sample length}}$$

was a better correction factor. The latter was used on this leg.

Two portable fluxgate magnetometers were also brought aboard during Leg 65 to check for potential sources of secondary magnetization. The GRAPE apparatus, diamond saws, and the drill press were examined, but no magnetic fields greater than 1 Oe were observed. A problem that had been mentioned on previous legs, the concentration of magnetic flux at the mouth of the magnetometer near the end of the mu-metal shields, was checked. The field around the top of the spinner magnetometer was mapped and was found to be no greater than the ambient field in the laboratory.

The normal laboratory procedure was to measure the NRM intensity and direction after demagnetization steps of 0, 25, 50, 75, 100, 125, and 150 Oe (and occasionally after further steps of 200, 300, and 400 Oe), and then to measure the weak field susceptibility. At each demagnetization step, the sample was demagnetized along each

of three orthogonal axes and care was taken to use the same orientation at each step of the procedure so that anhysteretic effects could be checked.

X-Ray Fluorescence Measurements

Whole-rock geochemical measurements were made during Leg 65 using the CNEXO XRF van on the *Glo-mar Challenger*. The oxides analyzed were SiO₂, Al₂O₃, Fe₂O₃, MgO, MnO, CaO, TiO₂, K₂O, and P₂O₅. These analyses were supplemented by shipboard measurements of H₂O⁺, H₂O⁻, and CO₂ and by shore-based measurements of Na₂O, Ni, Sr, and Zr. The analytical techniques used to determine the major oxides were similar to those used on Leg 37 and discussed in detail by Bougault (1977).

Sediment Description Conventions

The sediments recovered are described on standard sediment description forms using the conventions discussed below and the symbols presented in Figures 4, 5, and 6.

Core Disturbance

Unconsolidated sediments are often severely disturbed during the rotary drilling/coring process, and a complete gradation in the style of disturbance is observed with increasing sediment induration. An assessment of the degree and style of drilling deformation is made on-board ship for all cored material and is shown graphically on the core description sheets. The following symbols are shown in Figure 4:

- — — Slightly deformed; bedding contacts are slightly bent.
- · — · — Moderately deformed; bedding contacts have undergone extreme bowing.
- ~~~~~ Very deformed; bedding is completely disturbed, often showing symmetrical diapir-like structures.
- ○ ○ Soupy; water-saturated intervals have lost all aspects of original bedding and sediment cohesiveness.

Sedimentary Structures

Despite the potential for disturbance during drilling, many of the cores recovered show well-preserved sedimentary structures. The symbols recommended by an *ad hoc* committee of the JOIDES Sedimentary Petrology and Physical Properties Panel to represent such structures are shown in Figure 5.

Smear Slides

The lithologic classification of sediments is based on visual estimates of texture and composition in smear slides made on board ship. These estimates are of areal abundances on the slide and may differ somewhat from the more accurate laboratory determinations of grain size, carbonate content, and mineralogy. Experience has shown that distinctive minor components can be accurately estimated to ±1 or 2%, but that an accuracy of ±10% for major constituents is rarely attained. The carbonate content is especially difficult to estimate in

Primary Structures	
	Interval over which primary sedimentary structures occur
	Current ripples
	Micro-cross-laminae (including climbing ripples)
	Parallel laminae
	Wavy bedding
	Flaser bedding
	Lenticular bedding
	Slump blocks or slump folds
	Load casts
	Scour
	Graded bedding (NORMAL)
	Graded bedding (REVERSED)
	Convolute and contorted bedding
	Water escape pipes
	Mudcracks
	Cross-stratification
	Sharp contact
	Scoured, sharp contact
	Gradational contact
	Imbrication
	Fining-upward sequence
	Coarsening-upward sequence
	Bioturbation - minor (30% surface area)
	Bioturbation - moderate (30-60% surface area)
	Bioturbation - strong (more than 60% surface area)
Secondary Structures	
	Concretions
Compositional Symbols	
	Fossils in general (megafossils)
	Shells (complete)
	Shell fragments
	Wood fragments

Figure 5. Symbols for sedimentary structures.

smear slides, as is the amount of clay present. The locations sampled for smear-slide analysis are given on the core description sheets.

Sediment Induration

The determination of induration is highly subjective, yet field geologists have successfully made such distinctions for many years. The criteria of Moberly and Heath

(1971) are used for calcareous deposits; subjective estimates or behavior in core cutting are used for others.

1) Calcareous sediments:

Soft: Oozes have little strength and are readily deformed under either the fine or the broad blade of a spatula.

Firm: Chalks are partly indurated oozes; they are friable limestones readily deformed under the fingernails or the edge of a spatula blade.

Hard: Cemented rocks are termed limestones.

2) The following criteria are used for other sediments:

If the material is soft enough for the core to be split with a wire cutter, only the sediment name is used (e.g., silty clay; sand).

If the core must be cut by a saw, the suffix "stone" is used (e.g., silty claystone; sandstone).

Color

Colors are assigned according to standard Munsell or GSA color charts immediately after the cores are split (i.e., while still wet).

Sediment Classification

The basic classification system used on Leg 65 was devised by the JOIDES Panel on Sedimentary Petrology and Physical Properties and adopted for use by the JOIDES Planning Committee in March, 1974. The divisions used are necessarily artificial, and the classification is only a rough grouping of what we really find in nature. The classification scheme is thus descriptive and genetic implications are not intended. As noted above, the sediment and rock names used are defined solely on the basis of texture and composition determined on board ship from visual smear slide estimates. As in most such classification schemes, the texture is most important in the description of hemipelagic and nearshore sediments while the composition is important for sediments deposited under open marine conditions. Since the classification system is not comprehensive, a "Special Rock Type" category has been provided for rock types not covered.

The symbols used in the graphic lithology column of the sediment description form (Fig. 4) are shown in Figure 6. A single lithology will be represented by a single pattern. Some lithologies are represented by a grouping of two or more symbols. The symbols in this grouping may correspond to end-member sediment constituents, such as clay and nannofossil ooze. The ratio of one component to another may be represented in the graphic column by the symbols being presented in proportion to their percentages. For example, 20% of the column may have a clay symbol, whereas 80% of the column may have a nannofossil-ooze symbol. This would mean that the sample consists of approximately 80% nannofossils and 20% clay. The vertical lines which separate the symbols are shown in Figure 6 with their corresponding percentages and positions in the column. The format, style, and terminology used in the descriptive portion of the form are not specified beyond the minimal name assign-

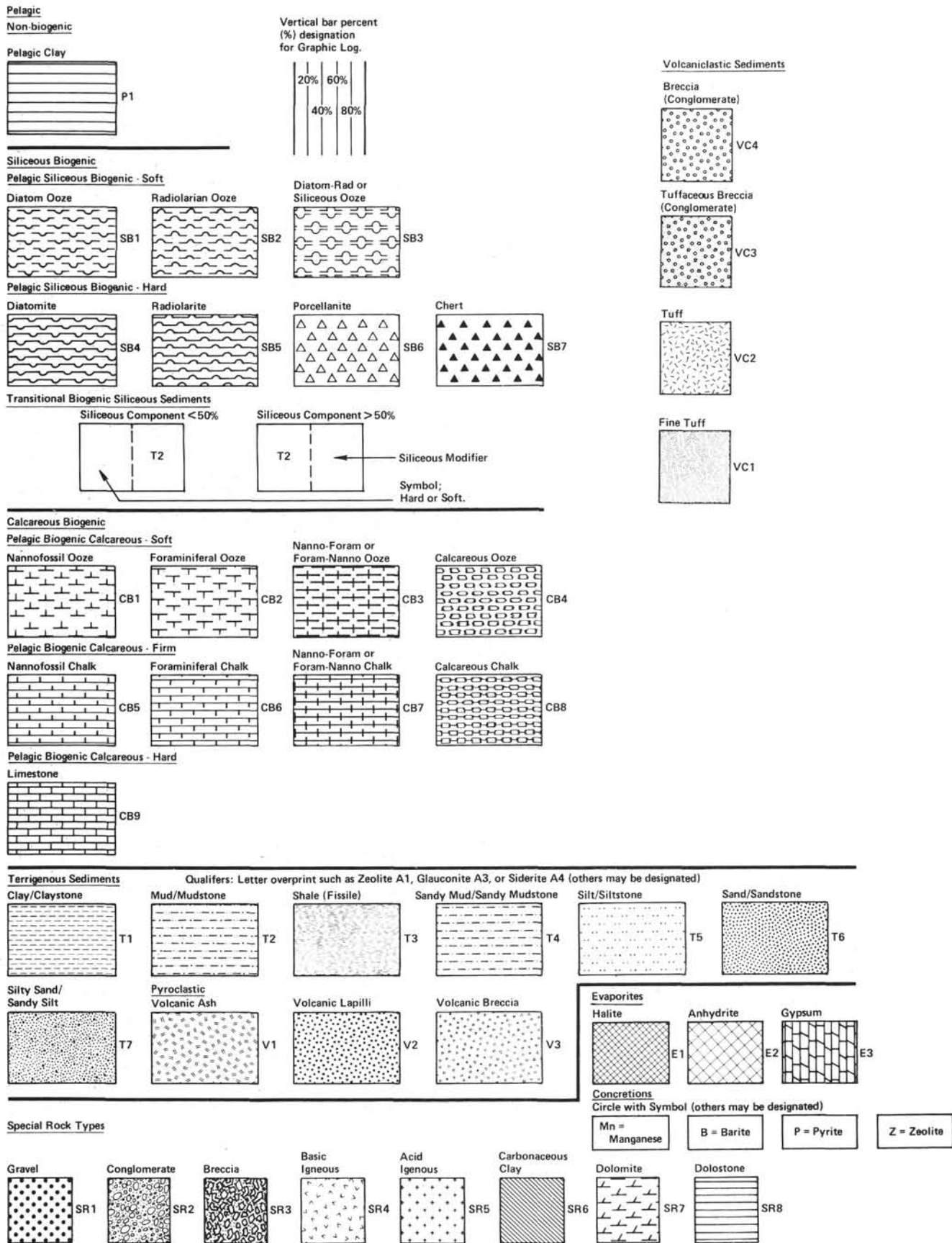


Figure 6. Graphic symbols used in lithologic classification.

ment derived using the classification scheme outlined below.

I. General Rules for Class Limits and Order of Components in a Sediment Name:

- A. The sediment assumes the names of those components present in quantities greater than 15%.
- B. Where more than one component is present, the component in greatest abundance is listed farthest to the right; other components are listed progressively to the left in order of decreasing abundance.
- C. The class limits are based on the percentage intervals given below for various sediment types.

II. Compositional Class Boundaries:

- A. CaCO₃ Content (determined by CaCO₃ bomb).

The compositional boundaries based on CaCO₃ content are 30% and 60%. Given the precision of the technique (5%) and the natural frequency distribution of CaCO₃ in oceanic sediments, these boundaries can be reasonably ascertained.

- B. Biogenic Opal Abundance.

The boundaries based on opal abundance (expressed as the percentage of siliceous skeletal material in smear slides) are 10%, 30%, and 50%. Smear slide estimates of identifiable siliceous skeletal material generally imply a significantly higher total opal abundance. The boundaries have been set to take this into account.

- C. Abundance of Authigenic Components (estimated from smear slides).

Zeolites, iron, and manganese micronodules, fish bones, and other indicators of very slow sedimentation are considered common if they represent 10% or more of the sediment. These components are quite conspicuous and a semiquantitative estimate is adequate. Because of the large difference in sedimentation rates, even a minor influx of calcareous, siliceous, or terrigenous material will dilute them to insignificance.

- D. Abundance of Terrigenous Detrital Material (estimated from smear slides).

The compositional boundary based on terrigenous detrital material is 30%.

- E. Qualifiers.

In general, constituents in the 10% to 30% range may be identified in the sediment name, e.g., vitric diatomaceous mud or vitric muddy diatomaceous ooze. If more than one such qualifier is used, they are listed in order of increasing abundance in the sediment. Components representing less than 5% of the sample are not used as qualifiers except in special cases.

III. Description of Sediment Types (Fig. 6):

A. Pelagic Clay.

These sediments are principally authigenic pelagic deposits that accumulate at very slow rates. The class is often termed brown clay or red clay, but since these terms are confusing, they are not recommended.

1. The boundary between pelagic clay and terrigenous sediments occurs where authigenic components (iron-manganese micronodules, zeolites, fish debris, etc.) become common in smear slides. (Note: because of the large discrepancy in accumulation rates, transitional deposits are exceptional.)
2. The boundary with siliceous biogenic sediments occurs where identifiable siliceous remains constitute less than 30% of the sample.
3. The boundary with calcareous biogenous sediments is gradational since the sequence observed generally passes from pelagic clay through siliceous ooze to calcareous ooze. There is one important exception: at the base of many oceanic sections, black, brown, or red clays occur directly on basalt and are overlain by, or grade upward into, calcareous sediments. Most of the basal clayey sediments are rich in iron, manganese, and metallic trace elements. For proper identification, they require more elaborate geochemical work than can be done on shipboard. These sediments are placed in the "Special Rock" category, but care should be taken to distinguish them from ordinary pelagic clays.

B. Pelagic Siliceous Biogenic Sediments.

These sediments are distinguished from the previous category by having more than 30% identifiable siliceous microfossils. They are distinguished from the following category by having a CaCO₃ content of less than 30%. There are two classes: pelagic biogenic siliceous sediments (containing less than 30% silt and clay) and transitional biogenic siliceous sediments (containing more than 30% silt and clay and more than 10% diatoms).

1. Pelagic Biogenic Siliceous Sediments.

- (a) Soft: Siliceous ooze (radiolarian ooze, diatom ooze, depending on dominant component).
- (b) Hard: Radiolarite, porcelanite, diatomite, and chert.
- (c) Qualifiers:
 - Radiolarians dominant—radiolarian ooze or radiolarite.
 - Diatoms dominant—diatom ooze or diatomite.

Where uncertain—siliceous (biogenic) ooze, chert, or porcelanite.

When containing more than 10% CaCO_3 , the qualifiers are as follows:

Indeterminate

carbonate: calcareous

Nannofossils

only: nannofossil

Foraminifers

only: foraminiferal

Both: nannofossil-foraminiferal or foraminiferal nannofossil, depending on dominant component.

2. Transitional Biogenic Siliceous Sediments.

(a) Diatoms less than 50% of sample:

Soft: Diatomaceous mud.

Hard: Diatomaceous mudstone.

(b) Diatoms more than 50% of sample:

Soft: Muddy diatom ooze.

Hard: Muddy diatomite.

(c) Radiolarian equivalents in this category are rare and can be specifically described.

3. Pelagic Biogenic Calcareous Sediments.

These sediments are distinguished from the previous categories by a CaCO_3 content in excess of 30%. There are two classes: pelagic biogenic calcareous sediments (containing less than 30% silt and clay) and transitional biogenic calcareous sediments (containing more than 30% silt and clay).

1. Pelagic Biogenic Calcareous Sediments.

(a) Soft: Calcareous Ooze.

(b) Firm: Chalk.

(c) Hard: Indurated Chalk.

The term limestone should be restricted to cemented rocks.

(d) Compositional qualifiers:

The principal components are nannofossils and foraminifers. One or two qualifiers may be used, depending on the percentage of foraminifers present:

%	Rock Name
<10	Nannofossil ooze, chalk, limestone
10-25	Foraminifer-nannofossil ooze
25-50	Nannofossil-foraminifer ooze
>50	Foraminifer ooze

Calcareous sediments containing more than 10% to 20% identifiable siliceous fossils carry the qualifier radiolarian, diatomaceous, or siliceous, depending on the quality of the identification; for example: radiolarian-foraminifer ooze.

2. Transitional Biogenic Calcareous Sediments.

(a) $\text{CaCO}_3 = 30\%$ to 60% : Marly calcareous pelagic sediments.

Soft: Marly calcareous (or nannofossil, foraminiferal, etc.) ooze (see below).

Firm: Marly chalk.

Hard: Marly limestone.

(b) $\text{CaCO}_3 > 60\%$: Calcareous pelagic sediments.

Soft: Calcareous (or nannofossil, foraminiferal, etc.) ooze (see below).

Firm: Chalk.

Hard: Limestone.

(Note: Sediments containing 10% to 30% CaCO_3 fall into other classes, denoted with the adjective "calcareous." If the CaCO_3 content is under 10%, it is ignored.)

D. Terrigenous and Volcanogenic Sediments.

1. Terrigenous Sediments.

Sediments falling within this category are subdivided into textural groups on the basis of the relative proportions of clay, silt, and sand. The size limits for these constituents are those defined by Wentworth (1922). Five major textural groups are recognized. They are defined according to the abundance of clay (>90%, 90% to 10%, and <10%) and the ratio of sand to silt (>1 or <1). Sands and sandstones may be subdivided further into very fine-, fine-, medium-, coarse-, and very coarse-grained categories according to their median grain size. Rocks coarser than sand size are treated as "Special Rock Types."

Numerous qualifiers may be applied to this group. These are usually based on minor constituents; for example: glauconitic, pyritic, feldspathic. For sands and sandstones, conventional divisions such as arkose and graywacke are acceptable, providing the scheme is properly identified. Clays, muds, silts, and sands containing 10% to 30% CaCO_3 are called calcareous.

2. Volcanogenic Sediments.

Pyroclastic rocks are described according to the textural and compositional scheme of Wentworth and Williams (1932). The textural groups are:

Volcanic breccia	> 32 mm
Volcanic lapilli	< 32 mm
Volcanic ash (tuff, if indurated)	< 4 mm

The compositions of pyroclastic rocks are described as vitric (glassy), crystalline, or lithic.

3. Clastic Sediments of Volcanic Origin.

These sediments are described in the same fashion as terrigenous sediments, with the dominant composition of volcanic grains noted where possible.

E. Special Rock Types.

The definition and nomenclature of rock types not included in the system described above are left to the discretion of the shipboard scientists, with the recommendation that they adhere as closely as possible to conventional terminology. In this category fall such rocks as:

Intrusive and extrusive igneous rocks (see below).

Evaporites (halite, anhydrite, gypsum, etc.).

Shallow water limestone (biostromal, biohermal, coquina, oolite).

Dolomite.

Gravels, conglomerates, and breccias.

Biostratigraphic Conventions

The scope of the paleontologic and biostratigraphic studies conducted on the Leg 65 sediments was limited by the youth of the material recovered and the relative paucity of markers. The zonal schemes used by the shipboard paleontologists were those of Be (1977) for the foraminifers; Martini (1971) for the nannofossils; and Benson (1966), Hays (1970), and Nigrini (1971) for the radiolarians.

BASEMENT DESCRIPTION CONVENTIONS

Core Forms

The description form used for sediments is too compressed to provide adequate information for hard rock sampling. Consequently, the form shown in Figure 7 is used for igneous and metamorphic rocks to permit more detailed graphic representation. Each column on this form covers a 1.5-meter section. Hand-specimen and thin-section descriptions as well as sample locations are presented for each section, while the corresponding chemical, magnetic, and physical properties data are presented in separate tables.

As in the case of the sediments, each basalt core is split into an archive and a working half, and the former is described and the latter sampled on shipboard. On the core forms, a visual representation of the archive half is presented in the left box. Closely spaced horizontal lines in this column indicate the location of Styrofoam spacers taped between basalt pieces inside the liner. The pieces are numbered sequentially from the top of each section, beginning with the number 1. Pieces are labeled on the rounded, not the sawed surface. Those which can be fit together before splitting are given the same number, but are consecutively lettered, as 1A, 1B, 1C, etc. Spacers were placed between pieces with different numbers, but not between those with the same number and different letters. In general, the addition of spacers

represents a drilling gap (no recovery). All pieces which are cylindrical and longer than the liner diameter were marked with orientation arrows pointing up, both on the archive and working halves. Special procedures were adopted to ensure that orientation was preserved through every step of the sawing and labeling process. All oriented pieces are indicated by upward-pointing arrows to the right of the graphic representation on the description forms. Since the pieces were rotated during drilling, it is not possible to sample for declination studies.

Samples were taken for various shipboard and shore-based measurements. The type of shipboard measurement and approximate location of the sample on which it was made are indicated in the column headed "Shipboard Studies" using the following codes:

X = X-ray fluorescence and CHN chemical analysis

M = Magnetic measurements

T = Thin section

S = Sonic velocity measurement

D = Density measurement

P = Porosity measurement

The presence of visible alteration is indicated qualitatively by diagonal lines in the box headed "Alteration." A number of the physical property (S, D, P) samples recovered on Leg 65 were permanently stored in seawater. These are indicated by a " \overline{W} " to the right of the alteration column.

Igneous Rock Classification

The igneous rocks drilled on Leg 65 were classified mainly on the basis of mineralogy and texture. Thin-section work in general added little new information to the hand-specimen classification.

Basalts are termed aphyric, sparsely phyric, moderately phyric, or phyric, depending on the proportion of phenocrysts visible under the binocular microscope ($\sim \times 12$). The basalts are called aphyric if phenocrysts are absent. In practice, this means that if one piece of basalt is found with one or two phenocrysts in a section where all other pieces lack phenocrysts, and no other criteria such as grain size or texture distinguish this basalt from the others in the section, then it is described as aphyric. A note on the rare phenocrysts is included in the general description, however. This approach enables us to restrict the number of lithologic units to those that appear to be clearly distinct.

Sparsely phyric basalts are those with 1% to 2% phenocrysts present in almost every piece of a given core or section. Clearly contiguous pieces without phenocrysts are included in this category, again with the lack of phenocrysts noted in the general description.

Moderately phyric basalts contain 2% to 10% phenocrysts. Aphyric basalts within a group of moderately phyric basalts are separately termed aphyric basalts.

Phyric basalts contain more than 10% phenocrysts. No separate designation is made for basalts with more than 20% phenocrysts; the proportion indicated in the core forms should be sufficient to guide the reader.

The basalts are further classified by phenocryst type, preceding the terms phyric, sparsely phyric, etc. For ex-

0 cm

1A

1B

2

XM

W

50

100

150

CORE/SECTION

Piece Number

Graphic Representation

Orientation

Shipboard Studies Alteration

Site, Core

Visual Description

Thin Section Description(s)

Code:

T = Thin section

D = Density

S = Sonic velocity

P = Porosity

X = XRF, CHN analysis

M = Paleomagnetic measurement

W = Stored in water

Figure 7. Description form for igneous rocks.

ample, a plagioclase-olivine moderately phyric basalt contains 2% to 10% phenocrysts, most of them plagioclase, but with some olivine.

REFERENCES

- Atwater, T., 1970. Implications of plate tectonics for the cenozoic tectonic evolution of western North America. *Geol. Soc. Am. Bull.*, 81:3513-3536.
- Bé, A. W. A., 1977. An ecological, zoogeographic and taxonomic review of Recent planktonic Foraminifera. In Ramsay, A. T. S. (Ed.), *Oceanic Micropaleontology* (Vol.1): New York (Academic Press), pp. 1-100.
- Benson, R. N., 1966. Recent Radiolaria from the Gulf of California [Ph.D. dissert.]. University of Minnesota, Minneapolis.
- Bougault, H., 1977. Major elements: Analytical chemistry on board and preliminary results. In Aumento, F., Melson, W. G., et al., *Init. Repts. DSDP*, 37: Washington (U.S. Govt. Printing Office), 643-657.
- Boyce, R. E. 1973. Appendix I. Physical property methods. In Edgar, N. T., Saunders, J. B., et al., *Init. Repts. DSDP*, 15: Washington (U.S. Govt. Printing Office), 1115-1128.
- Donnelly, T., Francheteau, J., Bryan, W., Robinson, P., Flower, M., Salisbury, M., et al., 1979. *Initial Reports of the Deep Sea Drilling Project*, V. 51, 52, 53: Washington (U.S. Government Printing Office).
- Hays, J. D., 1970. Stratigraphic and evolutionary trends of Radiolaria in North Pacific deep sea sediments. In Hays, J. D. (Ed.), *Geological Investigations of the North Pacific*, *Geol. Soc. Am. Mem.*, 126:185-218.
- Martini, E., 1971. Standard Tertiary and Quaternary calcareous nannoplankton zonation. *Second Planktonic Conf. Proc.: Rome* (Tecnoscienza), 739-785.
- Mathews, T., 1939. *Tables of the Velocity of Sound in Pure Water and Sea Water for Use in Echo Sounding and Sound Ranging*: London (Admiralty Hydrographic Department).
- Moberly, R., Jr., and Heath, G. R., 1971. Carbonate sedimentary rocks from the western Pacific: Leg 7, Deep Sea Drilling Project. In Winterer, E. L., Riedel, W. R., et al., *Init. Repts. DSDP*, 7, Pt. 2: Washington (U.S. Govt. Printing Office), 977-985.
- Müller, G., and Gastner, M., 1971. The "carbonate bomb," a simple device for the determination of the carbonate content in sediments, soils, and other materials, *N. Jahrb. Mineral. Mh.*, 10: 466-469.
- Nigrini, C. A., 1971. Radiolarian zones in the Quaternary of the equatorial Pacific Ocean. In Funnell, B. W., and Riedel, W. R. (Eds.), *The Micropaleontology of Oceans*: Oxford (Cambridge University Press), 443-461.
- Von Herzen, R., and Maxwell, A. E., 1959. The measurement of thermal conductivity of deep-sea sediments by a needle-probe method, *J. Geophys. Res.*, 46:1557.
- Wentworth, C. K., 1922. A scale of grade and class terms of clastic sediments, *J. Geol.*, 30:377.
- Wentworth, C. K., and Williams, H., 1932. The classification and terminology of the pyroclastic rocks. *Rept. Comm. Sed., Nat. Res. Council Bull.*, 89:19-53.